Quantum criticality

Subir Sachdev, and Bernhard Keimer

Citation: Physics Today **64**, 2, 29 (2011); doi: 10.1063/1.3554314
View online: http://dx.doi.org/10.1063/1.3554314
View Table of Contents: http://physicstoday.scitation.org/toc/pto/64/2
Published by the American Institute of Physics

feature article

Quantum criticality

Subir Sachdev and Bernhard Keimer

A phase transition brought on by quantum fluctuations at absolute zero may seem like an abstract theoretical idea of little practical consequence. But it is the key to explaining a wide variety of experiments.

Subir Sachdev is a professor of physics at Harvard University in Cambridge, Massachusetts. **Bernhard Keimer** is a director of the Max Planck Institute for Solid State Research in Stuttgart, Germany.

A significant part of modern physics research can be classified as the study of quantum matter. The aim is to describe the phases of large numbers of interacting particles at temperatures low enough that quantum mechanics plays a crucial role in determining the system's distinguishing characteristics. For electrons in solids, the needed "low" temperatures can be even higher than room temperature. Gases of trapped atoms require ultracold temperatures in the nanokelvin range. And through collisions of heavy nuclei, groups at particle accelerators are pursuing a quantum plasma of quarks with temperatures approaching those realized soon after the Big Bang. Remarkably, a common set of ideas on the phases of quantum matter applies across that wide range of energy scales.

Electron systems in solids are one of the best places to study quantum matter. With modern fabrication techniques, one can make an almost infinite variety of crystals, which provide a rich test bed for experimental investigations and theoretical descriptions of quantum phases. This article focuses on certain phase transitions the electrons undergo at the absolute zero of temperature. There are no thermal fluctuations at absolute zero. Instead, the transitions are driven by quantum fluctuations demanded by Heisenberg's uncertainty principle. The quantum critical point, where the transitions occur, is present only at absolute zero, but its influence nevertheless is felt in a broad regime of "quantum criticality" at nonzero temperatures, and it is the key to understanding a variety of experiments.

The most common quantum phases of electrons should be familiar to most readers: metals, with electrons occupying mobile plane-wave states; superconductors, with electrons forming Cooper pairs that can transport charge without dissipation; insulators, in which charge transport requires the exciting of electrons across an energy gap, which rarely happens at room temperatures; and semiconductors, which are essentially insulators with a smaller energy gap.

Such a classification focuses on the motion of the charge carried by the electron. However, the electron also has spin, and a study of the spin configuration in the electron wavefunction allows a more subtle classification of quantum phases. The rich variety of magnetic phases includes ferromagnets and antiferromagnets. The magnetic phases can be metals, superconductors, insulators, or semiconductors in their charge degrees of freedom.

Much recent experimental work has focused on so-called correlated-electron materials. In such materials, the electrons can occupy the atomic *d* or *f* orbitals, whose smaller spatial extent increases the importance of the Coulomb repulsion between the electrons, so the electrons' motion must be correlated to ensure that they stay apart from each other. Although most correlated-electron materials realize one of the common quantum phases above, many can be tuned between two or

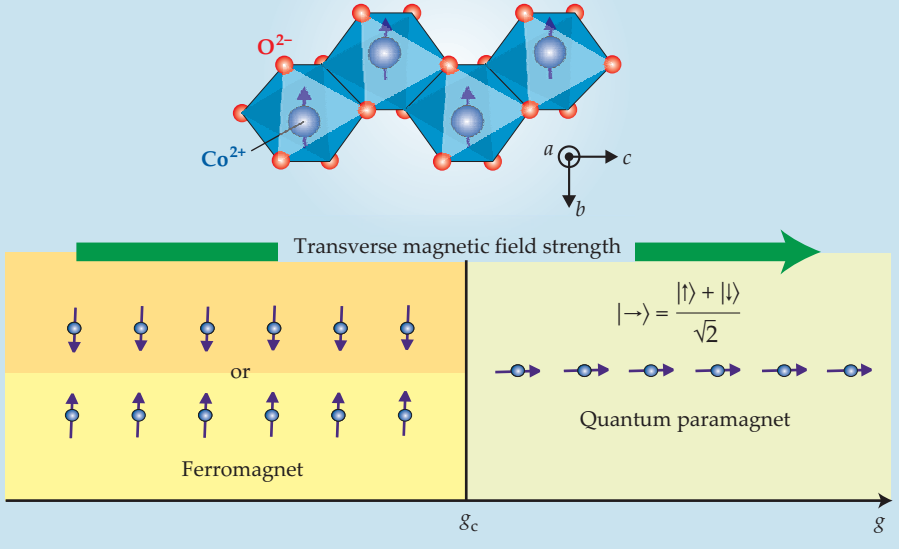

Figure 1. Cobalt niobate ($CoNb_2O_6$) provides an archetypal example of a quantum phase transition.[1] As the schematic of its crystal structure shows, the Co^{2+} ions have unpaired spins. In the absence of an applied magnetic field, the spins orient either parallel or antiparallel to a preferred axis in the *ac*-plane, forming a ferromagnet. When a transverse magnetic field is applied along the *b* axis and its strength *g* is increased, it eventually induces a different spin state, a quantum paramagnet with the spins aligned in the field direction. The spins undergo a second-order quantum phase transition at a critical field strength g_c.

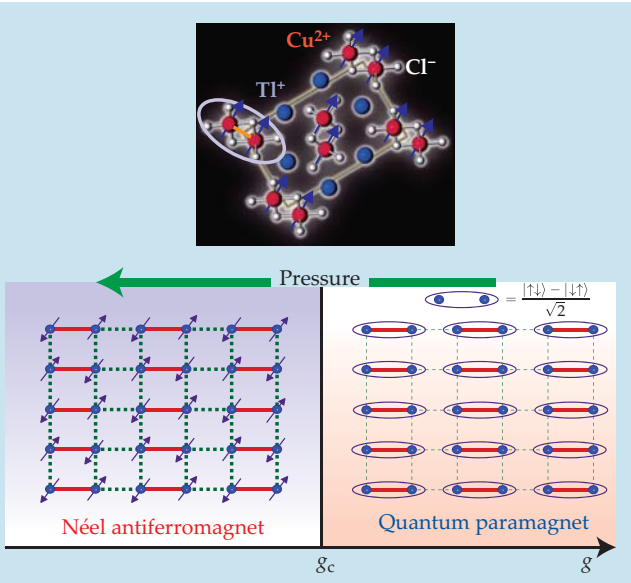

Figure 2. Thallium copper chloride ($TlCuCl_3$) exemplifies another quantum phase transition.[2] The Cu^{2+} ions boast active spin-½ states. At ambient pressure, the spins pair into dimers and form singlet bonds $(|\uparrow\downarrow\rangle - |\downarrow\uparrow\rangle)/\sqrt{2}$, as indicated by the ellipsis (top). The behavior is similar to that of a so-called dimer antiferromagnet on a square lattice. The solid red lines represent strong spin interaction with a positive exchange coupling $J > 0$, while the dashed green lines have a weaker exchange coupling J/g, with $g \geq 1$. The ground state of $TlCuCl_3$ is similar to the dimerized, large-g ground state of the dimer antiferromagnet, which behaves like a quantum paramagnet (right). For $TlCuCl_3$, g is inverse pressure. As the pressure increases and g decreases, $TlCuCl_3$ undergoes a quantum phase transition to Néel antiferromagnetic order, in which neighboring spins are antiparallel. In the dimer antiferromagnet model, the transition to Néel order occurs at a quantum critical point $g = g_c$.

more phases by varying an external parameter. The parameter could be the pressure applied to the solid, the strength of an external magnetic field, or the density of electrons in the solid (which can be controlled, for example, by the concentration of dopant ions). Temperature isn't in this list of external parameters: We are considering changes in the ground state of the electrons and are not yet interested in the thermal excitations above it. In this article we will generically refer to the tuning parameter as g. As g is varied, there is the possibility at some critical point $g = g_c$ of a quantum phase transition: a qualitative change in the ground-state wavefunction of a large many-body system on smoothly changing one or more coupling constants in its Hamiltonian.

Sometimes, the transition between the two phases can involve sudden jumps in physical properties; such a first-order quantum transition is analogous to a first-order thermally driven phase transition, like water boiling to steam. More interesting and quite common, however, is the continuous transition, in which the change is more gradual.

A key feature of a second-order quantum phase transition is the special nature of the ground state precisely at $g = g_c$. Far away from the quantum critical point, the system is usually in one of the states mentioned above, such as a metallic antiferromagnet, for which one can write down a straightforward wavefunction involving a product of simple configurations of all the electrons. For a first-order transition, those simple states are found on both sides of the transition all the way to $g = g_c$, and the quantum state just jumps from one to the other upon crossing the transition. For a continuous transition, in contrast, the wavefunction at $g = g_c$ is very different from a product state: It is a complex quantum superposition of an exponentially large set of configurations fluctuating at all length scales. In modern parlance, the critical-point wavefunction has long-range quantum entanglement. Albert Einstein, Boris Podolsky, and Nathan Rosen emphasized the peculiar nonlocal nature of quantum entanglement in their famous 1935 thought experiment on a single pair of electrons; a similar entanglement appears here in a system of a very large number of electrons and between electrons separated at all length scales.

Quantum-critical states are among the most complicated quantum states ever studied, and describing them efficiently is an important goal of theoretical studies of quantum criticality. In almost all cases, one cannot even explicitly write down the critical wavefunction; instead, one must usually resort to tools from quantum field theory or from numerical simulations to extract the subtle quantum correlations between the electrons.

The quantum-critical state at $g = g_c$ is defined by the ground-state wavefunction, so, strictly speaking, it is present only when the temperature T is at absolute zero. Thus, from an experimental perspective, it may seem that a continuous quantum phase transition, and its exotic entangled critical point, is an abstract theoretical idea of little practical interest. However, as described below, the influence of the critical point extends over a wide regime in the $T > 0$ phase diagram. That regime of quantum criticality is the key to explaining a wide variety of experiments.

The quantum Ising chain

Two paradigmatic examples from recent experiments illustrate quantum phase transitions and quantum criticality. Both examples are in insulators, so the electron charge is localized and we can focus attention solely on the orientation of the electron spins on different sites in the crystal lattice.

In cobalt niobate, $CoNb_2O_6$, only the total electronic spin on the Co^{2+} ion is able to choose its orientation. Because of spin–orbit effects, the Co^{2+} spins have a lower energy when their spins are either parallel or antiparallel to a preferred crystalline axis; such spins are referred to as Ising spins. We denote the two possible electronic spin states on the Co^{2+} ion at site j by $|\uparrow\rangle_j$ and $|\downarrow\rangle_j$. In quantum computing terminology, each Co^{2+} ion realizes a qubit. The spin Hamiltonian of $CoNb_2O_6$ has a coupling between neighboring spins along one-dimensional zigzag chains in the crystal, shown in figure 1, so that the spins prefer to be parallel to each other. Consequently, in its ground state, $CoNb_2O_6$ is a ferromagnet, with all spins parallel (figure 1, left). There are two possible ferromagnetic ground states:

$$|\Uparrow\rangle = \prod_{j=1}^{N} |\uparrow\rangle_j \quad \text{or} \quad |\Downarrow\rangle = \prod_{j=1}^{N} |\downarrow\rangle_j \,, \tag{1}$$

where N is the total number of spins in the chain. The ground states are simple product states, as expected far from a quantum critical point. The crystal chooses one of the two states depending on small external perturbations. That choice between the states breaks the reflection symmetry across the xy-plane, under which $|\uparrow\rangle_j$ is interchanged with $|\downarrow\rangle_j$.

One can drive a quantum phase transition in $CoNb_2O_6$ by applying a magnetic field transverse to the preferred crystalline axis, as was done recently by Radu Coldea and colleagues.[1] The strength of the transverse field is the tuning parameter g. As $g \to \infty$, a ground state very different from

Box 1. Excitations in the dimer antiferromagnet

The two noncritical ground states of the dimer antiferromagnet in figure 2 have very different excitation spectra. In the quantum paramagnet regime, let $|s\rangle_i$ denote the spin-singlet valence bond $(|\uparrow\downarrow\rangle - |\downarrow\uparrow\rangle)/\sqrt{2}$ on dimer i. The ground state is approximately

$$|G\rangle = \prod_i |s\rangle_i .$$

Any one dimer, say i, can be excited to one of three possible triplet states $|t_m\rangle_i$ with spin $S = 1$:

$$|t_1\rangle = |\uparrow\uparrow\rangle , \quad |t_0\rangle = \frac{|\uparrow\downarrow\rangle + |\downarrow\uparrow\rangle}{\sqrt{2}} , \quad |t_{-1}\rangle = |\downarrow\downarrow\rangle .$$

A collection of N_d excited dimers can be viewed in momentum space as "triplon" particles of momentum $\mathbf{k}$,

$$|t_m(\mathbf{k})\rangle = \frac{1}{\sqrt{N_d}} \sum_i e^{i\mathbf{k}\cdot\mathbf{r}_i} |t_m\rangle_i \prod_{j\neq i} |s\rangle_j ,$$

where $\mathbf{r}_i$ is the position of excited dimer i. One can form wavepackets to localize the triplons in space.

In the Néel state, the ground state is the staggered spin configuration shown in figure 2. Spin-wave excitations, in which the orientation of the local Néel order is rotated slowly in space, have nearly zero energy. A second class of excitations are oscillations in the magnitude of the average local magnetization; those excitations are the analogue of the Higgs particle.

The excitations of the dimer antiferromagnet thallium copper chloride ($TlCuCl_3$) have been measured by Christian Rüegg and colleagues using neutron scattering[2] and are shown in the figure. Applied pressure serves as the inverse of the tuning parameter g. The blue dots show the energy of the triplon excitations of the quantum paramagnet. In the Néel regime, the white circles are the spin-wave excitations, and the red circles are the magnetization oscillations.

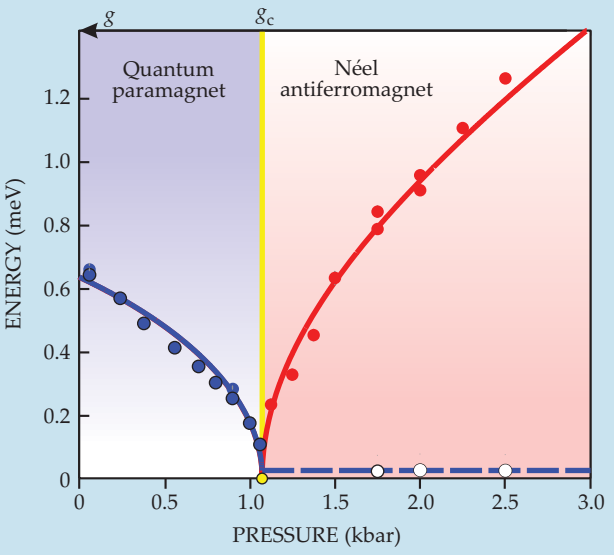

equation 1 must appear. Because of the Zeeman coupling, all spins must orient parallel to the applied field; for a field in the x-direction, that leads to the unique ground state

$$|\Rightarrow\rangle = \prod_{j=1}^{N} |\rightarrow\rangle_j , \quad \text{where} \quad |\rightarrow\rangle_j \equiv \frac{|\uparrow\rangle_j + |\downarrow\rangle_j}{\sqrt{2}} . \qquad (2)$$

Expanding the product in equation 2 yields an equal superposition of all 2^N states of the N qubits, a fact that is put to good use in quantum computing. Unlike the states in equation 1, the state in equation 2 is invariant under the interchange of $|\uparrow\rangle_j$ and $|\downarrow\rangle_j$, so it does not break the xy-plane reflection symmetry. It is not a ferromagnet but instead is termed a quantum paramagnet.

It is not possible to vary g and smoothly connect the states in equation 1, obtained for $g = 0$, to the state in equation 2, obtained for $g \to \infty$. That is clear from the fact that reflection symmetry is broken in the former states but not in the latter. Thus there must be a point of nonanalyticity in g, where the ferromagnetic moment in the ground state vanishes and symmetry is restored; that is the quantum critical point, g_c.

We can now describe the continuous quantum phase transition, and the nature of the ground-state wavefunction as a function of g, more completely. The simple product wavefunctions in equations 1 and 2 describe $g \ll g_c$ and $g \gg g_c$. Precisely at $g = g_c$, the quantum-critical state is a highly nontrivial quantum superposition of all 2^N spin configurations, and correlations between spins decay as a power law of distance. The alert reader will notice that $|\Rightarrow\rangle$ also involves a superposition of all 2^N states in the up–down basis, but it is an equal-weight superposition of all the states, so it can be written as a simple product state in the left–right basis. In contrast, there is no local basis for which the quantum-critical state at $g = g_c$ takes a simple form—it is quantum entangled.

Points not too far from $g = g_c$ are characterized by a crucial length scale, the ground-state spin coherence length ξ. Averaged over length scales larger than ξ, the wavefunction reduces to the simple product form appropriate for $g \gg g_c$ (when $g > g_c$) or $g \ll g_c$ (when $g < g_c$). But at length scales smaller than ξ, the wavefunction looks like the entangled state at $g = g_c$; in a sense, at scales shorter than ξ the electrons have not "decided" which side of the quantum phase transition they are on, so they acquire the intricate characteristics of the critical point between the phases. The value of ξ varies as a function of g, and a central characteristic of the continuous quantum phase transitions we consider here is that ξ diverges as $|g - g_c|$ approaches zero.

The changes in the ground-state wavefunction as a function of g are accompanied by corresponding changes in the nature of the low-energy excitations. By detecting those excitations in neutron scattering experiments[1] (see PHYSICS TODAY, March 2010, page 13), Coldea and coworkers demonstrated the existence of a continuous quantum phase transition in $CoNb_2O_6$.

Dimer antiferromagnet

Our second example, the dimer antiferromagnet, is realized in thallium copper chloride, $TlCuCl_3$. In that material, each Cu^{2+} ion has an unpaired, localized electron spin. Let $\mathbf{S}_j$ be the spin-½ operator for site j, and let the exchange couplings J_{ij} characterize the strength of the spin–spin interactions between the Cu^{2+} ions. The spins are then described by the Hamiltonian

$$H = \sum_{i<j} J_{ij} \mathbf{S}_i \cdot \mathbf{S}_j . \qquad (3)$$

A key feature in $TlCuCl_3$ is that $J_{ij} \geq 0$: The couplings are antiferromagnetic and prefer *anti*parallel spins, unlike the spin–spin couplings of the Ising chain above. Furthermore, they

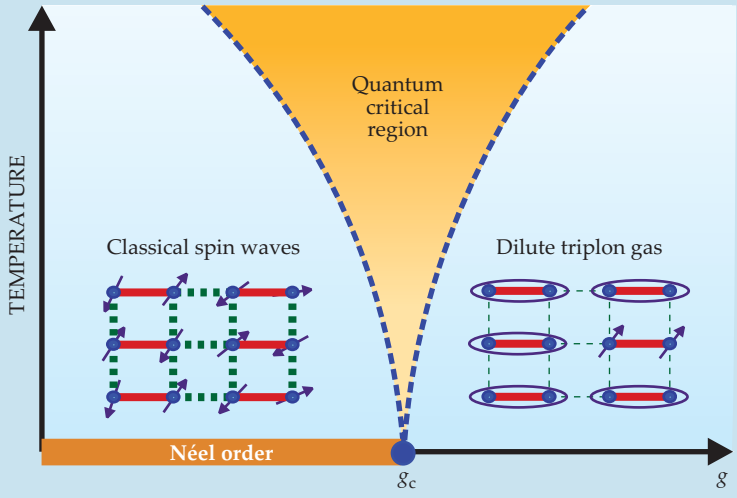

Figure 3. Quantum criticality extends to nonzero temperatures. Sketched here is the phase diagram for the model in figure 2. In the blue region for small g, thermal effects induce spin waves that distort the Néel antiferromagnetic ordering. For large g, thermal fluctuations break dimers in the blue region and form quasiparticles called triplons, as described in box 1. The dynamics of both types of excitations can be described quasi-classically. Quantum criticality appears in the intermediate orange region, where there is no description of the dynamics in terms of either classical particles or waves. Instead, the system exhibits the strongly coupled dynamics of nontrivial entangled quantum excitations of the quantum critical point g_c.

are dimerized: Each spin j is coupled strongly to only a single partner spin; the couplings to all other spins are smaller. Figure 2 presents a simple model of a dimer antiferromagnet that has couplings J and J/g, with $g \geq 1$.

In that model, the ground state for $g = 1$ has Néel (or antiferromagnetic) order, with the spins polarized in a checkerboard pattern. Each spin has a definite orientation—the symmetry of spin rotations has been broken. The state's wavefunction again has a simple product form. The Néel ground state is the analogue of the ferromagnetic state of the Ising chain, except that now the spins are polarized in a staggered spatial pattern. Each up spin has down neighbors (and vice versa), so each term in H is negative.

Now, the ground state for $g \to \infty$ is very different. At $g = \infty$, the couplings between different dimers vanish and the Hamiltonian decouples into a sum over independent pairs of spins. We can easily find the ground state for each dimer of spins: It is the singlet valence bond, $(|\uparrow\downarrow\rangle - |\downarrow\uparrow\rangle)/\sqrt{2}$, which is rotationally invariant. Although the two spins are always antiparallel, they are equally likely to point in any direction in spin space. The ground state of the full system at $g = \infty$ is then a product over such singlet valence bonds, as illustrated in figure 2, and is also a quantum paramagnet.

The remaining discussion for H parallels that for the Ising chain. There is Néel order, with broken spin-rotation symmetry, for a range of g. Spin-rotation symmetry is restored at a quantum critical point $g = g_c$, beyond which the ground state is a spin-singlet quantum paramagnet. There is a continuous transition at g_c, where the ground state has nontrivial entanglement between the spins at all length scales.

The ground states of figure 2 have been observed by Christian Rüegg and collaborators[2] in $TlCuCl_3$, with g tuned by applied pressure. The distinct low-energy excitations of the two noncritical ground states have been detected in neutron scattering and are described in box 1.

Quantum criticality

We turn, at last, to the experimental significance of the isolated quantum critical point at $g = g_c$, on which we have lavished much attention above. For that, we need to consider the influence of a nonzero temperature on the quantum phase transition in the ground state. As we will see, the transition leaves a clear fingerprint on a large portion of the $T > 0$ phase diagram.[3]

Figure 3 sketches the phase diagram in the Tg-plane for the dimer antiferromagnet of figure 2. Above the noncritical ground states, the temperature will excite the states described in box 1, as shown in the blue regions of figure 3. The dynamics of the waves or particles can be described by a quasi-classical model. Box 2 shows the corresponding phase diagram for the Ising chain.

As noted above, close to $g = g_c$ the ground-state wavefunction has the entangled critical form at lengths smaller than ξ; at longer lengths, the wavefunction has the noncritical product form. At finite temperatures, the system has another characteristic length: $\hbar c/k_B T$, the characteristic de Broglie wavelength of the excitations at the quantum critical point g_c (here, c is the spin-wave velocity). When $\xi < \hbar c/k_B T$ (the blue regions of figure 3), the wavefunction assumes the product form at a length scale shorter than that at which thermal effects are manifested. So thermal fluctuations excite the noncritical wave and particle states.

The novel quantum-critical region, colored orange in figure 3, emerges in the opposite limit, when $\hbar c/k_B T < \xi$. Since ξ diverges as $|g - g_c|$ vanishes, the region has a characteristic fan shape. Remarkably, and somewhat paradoxically, the importance of quantum criticality increases with increasing T, far beyond the isolated quantum critical point at $T = 0$. (Of course, once the thermal energy is as large as the spin–spin coupling J, all the arguments here break down; the phase diagram in figure 3 applies only when T remains smaller than J.) Because the de Broglie wavelength is shorter than ξ, thermal fluctuations act directly on the quantum-critical entangled state. Thus we need a theory of the excitations of the complex critical state and the manner in which they interact with each other.

Describing the dynamics of quantum criticality is a major challenge and the subject of much current research. None of the analytic, semiclassical, or numerical methods of condensed-matter physics yield accurate results, except for some special systems in one spatial dimension. But one key characterization that applies to essentially all strongly interacting quantum critical points in two or more spatial dimensions relates to the thermal equilibration time τ_{eq}. That is the time it takes for the system to relax back to local thermal equilibrium after it is disturbed by an arbitrary external perturbation. In the quantum-critical region,[4]

$$\tau_{eq} = C_{eq} \frac{\hbar}{k_B T}, \qquad (4)$$

where C_{eq} is a dimensionless universal number: It is independent of the specific microscopic form of the Hamiltonian

Box 2. Thermal excitations in the quantum Ising chain

The one-dimensional quantum Ising chain, as found in cobalt niobate ($CoNb_2O_6$), has the attraction that many aspects can be solved theoretically for nearest-neighbor interactions, even at finite temperature. This plot shows the normalized value of the temperature derivative of the inverse spin correlation length, $d\xi^{-1}/dT$; that quantity is a measure of the strength of interactions between thermal excitations. The derivative has a temperature dependence similar to that of the temperature derivative of the inverse thermal equilibration time, τ_{eq}^{-1}, of nonintegrable strongly interacting quantum critical points. In the quantum-critical regime, $\tau_{eq}^{-1} \sim T$ and the system approaches a nearly perfect fluid. Outside of the quantum-critical region, the system adopts different spin configurations. Excitations in the ferromagnetic regime, $g < g_c$, have the two spin orderings of equation 1, separated by domain walls; for $g > g_c$, the paramagnetic state of equation 2 has reversed-spin excitations that are antiparallel to the applied magnetic field.

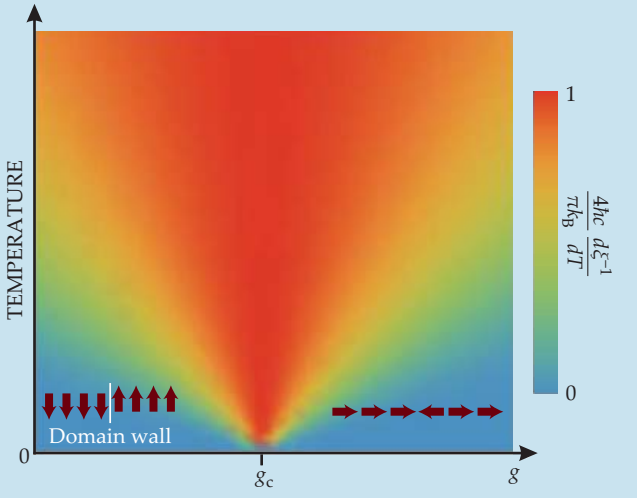

and depends only upon general features such as the dimensionality of the system and the global spin symmetries of the Hamiltonian. All other regimes of quantum dynamics, such as the blue regions of figure 3, have much longer values of τ_{eq}. Thus quantum criticality is distinguished by its ability to relax to thermal equilibrium in the *shortest possible time*. Furthermore, that time is the shortest allowed by quantum mechanics, so a system in the quantum-critical region can be viewed as a nearly perfect fluid. (For more on nearly perfect fluids, see the special issue of PHYSICS TODAY, May 2010.)

Equation 4 has important consequences for the spin fluctuation spectrum in the quantum-critical region, as measured by neutron scattering experiments. The spectral intensity for an excitation with energy $\hbar\omega$ depends only on the thermal energy k_BT and not on any energy (like the exchange interaction J) in the Hamiltonian. That sole dependence on k_BT is unique to the quantum-critical region; it does not hold for the blue regions in figure 3. Measurements of the spectrum in the orange region at different temperatures fall on the same curve when plotted as a function of $\hbar\omega/k_BT$. Precisely such a spectrum has been observed for spin-½ ions in 1D and geometrically frustrated 2D lattices and in copper oxide superconductors and rare-earth intermetallic compounds near the quantum phase transition to antiferromagnetism.[5]

The motions of conserved quantities like spin, charge, or momentum also enjoy a remarkable universality under quantum criticality. The collisional and dissipative processes that establish local equilibrium are similar to those that determine the coefficients of various friction forces impeding the motion of conserved quantities. Consequently, it follows from the universality of equation 4 that the friction coefficients are also universal. For example, for the linear momentum of a quantum-critical fluid, the associated "friction" is measured by the shear viscosity η, given by

$$\frac{\eta}{s} = C_m \frac{\hbar}{k_B}, \qquad (5)$$

where s is the entropy density and C_m is another universal dimensionless number of order unity.[6] It has so far not been possible to measure the value of η for interacting electrons in quantum matter. However, such measurements are more natural in ultracold atoms and the quark–gluon plasma and have been measured in those systems[7] (see the articles by John Thomas and by Barbara Jacak and Peter Steinberg, PHYSICS TODAY, May 2010, pages 34 and 39). The universality of quantum-critical transport also extends to charge and spin transport and to their associated conductivities.

In some simpler cases, mainly in insulators, the quantum critical point at $g = g_c$ is described by a mathematical framework known as a conformal field theory (CFT). Well known in statistical mechanics and string theory, CFTs enjoy a large group of spacetime symmetries, including relativistic invariance and scale invariance. In particular, the simple square-lattice model in figure 2 with the Hamiltonian in equation 3 has a critical point described by a CFT in which the velocity of light is replaced by the spin-wave velocity. The analytic understanding of quantum criticality is most advanced for those critical points described by CFTs. That is partly due to the discovery of the so-called AdS/CFT correspondence, which relates quantum criticality to dynamics near the horizon of a black hole in a particular spacetime geometry, known as anti–de Sitter (AdS) space, that has one more spatial dimension than the CFT (see the article by Igor Klebanov and Juan Maldacena, PHYSICS TODAY, January 2009, page 28). Remarkably, the characteristic quantum-critical time in equation 4 is mapped onto the damping time of quasi-normal modes of the gravitational, electromagnetic, and other fields around the black hole, with T mapped onto the temperature of Hawking radiation of the black hole. In the past two years, much research has gone toward extending such string-theory-inspired ideas to quantum criticality not associated with a relativistic CFT, and some very promising results are being obtained.[8]

Metals and superconductors

We have discussed insulators so far, but the majority of the experimental work on novel quantum phases and their quantum phase transitions has focused on metallic compounds. The landscape of crystalline materials combining three or more elements is vast, and new experimental discoveries continue unabated. Among the most celebrated examples are the copper oxide compounds (the cuprates), such as $La_{2-x}Sr_xCuO_4$, that display high-temperature superconductivity. In a particular stoichiometric limit, cuprates are good insulators that display Néel order similar to that in $TlCuCl_3$. However, by varying the relative concentration of elements, one can dope the materials with mobile charge carriers and eventually, for sufficiently high dopant densities, turn them into good metals. Along the way, high-temperature superconductivity is

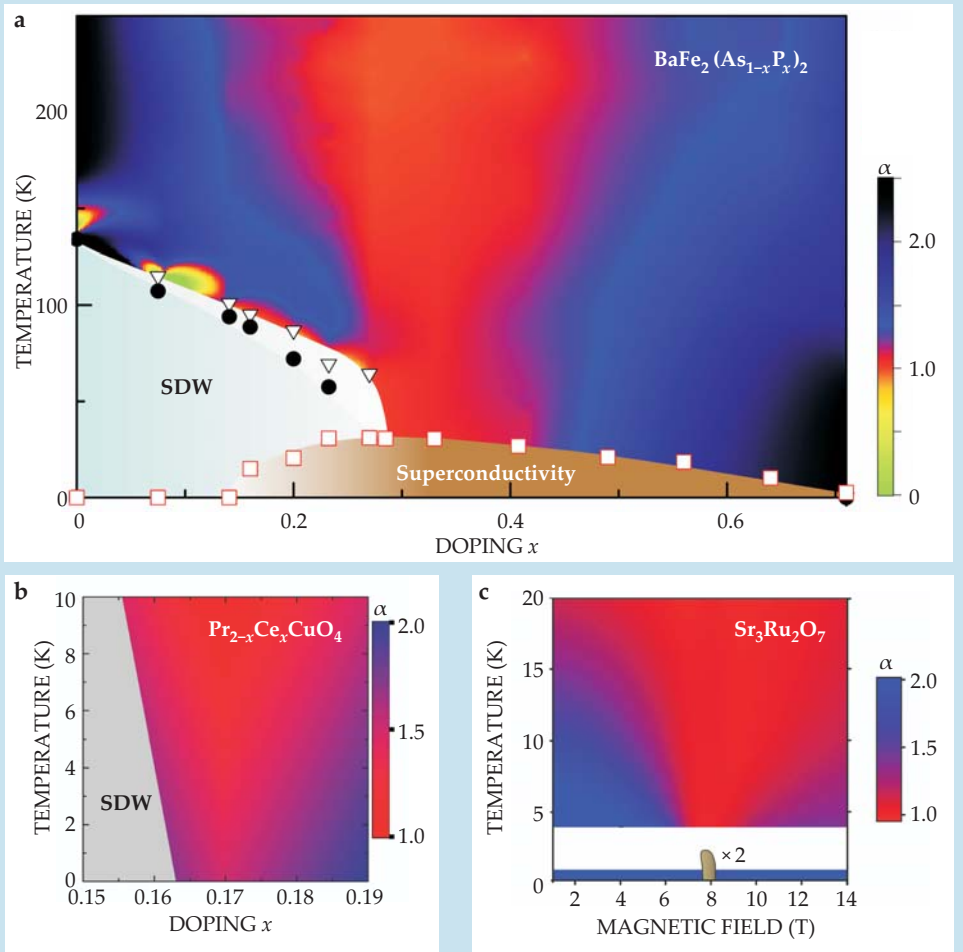

Figure 4. Resistivity plots for various correlated-electron materials. The colors represent the exponent α that describes the temperature dependence of the resistivity ρ: $\rho \sim \rho_0 + AT^{\alpha}$. The fan shapes of so-called strange-metal behavior, where $\alpha \approx 1$, can be interpreted as regions of quantum criticality. **(a)** The iron-based pnictide compound $BaFe_2(As_{1-x}P_x)_2$ can be doped with charge carriers. For low doping and low temperatures, the material exhibits a spin-density wave (SDW)—that is, antiferromagnetic order in a metal. For higher doping, the material turns superconducting at low temperatures. The shape symbols show the experimentally measured phase boundaries.[11] **(b)** The electron-doped copper oxide superconductor $Pr_{2-x}Ce_xCuO_4$ behaves similarly. Here its superconductivity has been suppressed by an applied magnetic field.[12] **(c)** In the ruthenate $Sr_3Ru_2O_7$ at low temperature near the critical magnetic field (brown region), the electronic motion breaks the underlying crystal symmetry and instead has an ordering resembling nematic liquid crystals.[17]

observed. Such changes clearly set up numerous possibilities for interesting quantum phase transitions. More recent examples are the iron-based pnictide compounds such as $BaFe_2(As_{1-x}P_x)_2$, which display a similar set of phases, including superconductivity.

At the heart of the quantum phase transitions of those materials is a new ingredient not found in insulators: the Fermi surface. In the simplest theory of a metal, electrons occupy plane-wave states that are eigenstates of momentum, and the set of lowest-energy occupied states is bounded in momentum space by the Fermi surface. That surface is of great physical significance because it is the locus of crucial low-energy excitations of the metal. Electrons move from occupied states just below the Fermi surface to unoccupied states just above it. When a metal undergoes a quantum phase transition, such as the onset of Néel order, the shape of the Fermi surface changes significantly. So a theory of the Néel-ordering quantum critical point in a metal must account not only for the collective spin fluctuations—spin waves and triplons—associated with the onset of Néel order, just as in an insulator, but also for the concomitant change in shape of the Fermi surface and the associated changes in the occupied electron states.

Much theoretical effort has been expended in the past two decades in trying to understand the simplest paradigms of quantum phase transitions in metals.[9] Some theories appear to be reasonably well understood in three spatial dimensions. But the 2D case is of central importance, because most of the interesting experimental examples of metallic quantum phase transitions are in compounds, such as the copper- and iron-based materials just noted, in which the electron motion is primarily along single crystalline planes. All current theories have very strongly coupled spin and charge transitions in two spatial dimensions, and only limited results are available so far.[10]

In experimental studies of quantum phase transitions with Fermi-surface changes in 2D metals, a ubiquitous feature is so-called strange-metal behavior. One hallmark of the strange-metal regime is that the electrical resistivity ρ is linearly proportional to the temperature T. That behavior is in stark contrast to the predictions of the standard Fermi-liquid theory of metals, which has $\rho \sim T^2$ at low temperatures.

Figure 4 shows several examples of strange-metal behavior. It is found in regions shaped very much like the quantum-critical regions of the insulators discussed above. That similarity supports the interpretation of strange metals as the quantum-critical regions of the quantum phase transitions involving changes in the Fermi surfaces of metals. In the phase diagrams[11,12] of iron-based $BaFe_2(As_{1-x}P_x)_2$ in figure 4a and the electron-doped cuprate $Pr_{2-x}Ce_xCuO_4$ in figure 4b, it is also clear that the Fermi-surface change is linked to the onset of antiferromagnetism. Curiously, the phase diagram[13] for the hole-doped cuprate $La_{2-x}Sr_xCuO_4$ could be interpreted in terms of a novel quantum-critical phase, in which the long-range entangled ground state at absolute zero exists over a small but finite range of g rather than at a single critical point g_c.

Another notable feature of figure 4 is that at low temperatures, "bare" quantum criticality is invariably preempted by

another phase. The most prominent and common example is the appearance of unconventional superconductivity, as is found in the copper oxides and the iron pnictides. Whereas in traditional superconductors a Cooper pair's electronic wavefunction is isotropic in space, in unconventional superconductors the pair wavefunction has a nontrivial spatial dependence and changes sign between different regions of momentum space. Signatures of such a sign change have been found in numerous beautiful experiments. The theory of antiferromagnetic quantum criticality in metals also has clear signatures of instabilities to such unconventional superconductivity near the quantum critical point.

Another interesting instability of metallic quantum criticality is the so-called electronic nematic state. In that state, electron motion spontaneously breaks the crystal's rotation symmetry in a manner analogous to the onset of liquid-crystalline order in complex fluids. The electronic nematic state was first identified[14] in $Sr_3Ru_2O_7$ (figure 4c), and evidence has since been found for substantial nematic correlations in the copper- and iron-based superconductors close to their antiferromagnetically ordered phases.[15]

The nucleation of new types of quantum order near quantum phase transitions makes the transitions an important resource for materials physics: They are guiding the search for new material properties of potential technological importance. For the future, we need a comprehensive theory of such multiple-ordering phenomena and their interplay with electronic excitations near the Fermi surface. In particular, a full understanding of nonlinear effects between various orders is needed—how one static or fluctuating order enhances or suppresses other orderings. That understanding will help describe the phase diagrams in a strong magnetic field, which can provide a second tuning parameter in some systems.[16] Such experimental phase diagrams have emerged as key tests of theoretical proposals. With the rapid progress over the past few years, we are well on our way toward a systematic description of quantum criticality and competing orders in metals with strong electronic correlations.

References

1. R. Coldea et al., *Science* **327**, 177 (2010).
2. C. Rüegg et al., *Phys. Rev. Lett.* **100**, 205701 (2008).
3. S. Chakravarty, B. I. Halperin, D. R. Nelson, *Phys. Rev. B* **39**, 2344 (1989).
4. S. Sachdev, J. Ye, *Phys. Rev. Lett.* **69**, 2441 (1992); A. V. Chubukov, S. Sachdev, J. Ye, *Phys. Rev. B* **49**, 11919 (1994).
5. B. Lake et al., *Nat. Mater.* **4**, 329 (2005); J. S. Helton et al., *Phys. Rev. Lett.* **104**, 147201 (2010); B. Keimer et al., *Phys. Rev. B* **46**, 14034 (1992); G. Aeppli et al., *Science* **278**, 1432 (1997); A. Schröder et al., *Nature* **407**, 351 (2000).
6. P. K. Kovtun, D. T. Son, A. O. Starinets, *Phys. Rev. Lett.* **94**, 111601 (2005).
7. E. Shuryak, *Physics* **3**, 105 (2010).
8. J. McGreevy, *Physics* **3**, 83 (2010).
9. J. A. Hertz, *Phys. Rev. B* **14**, 1165 (1976); T. Moriya, *Spin Fluctuations in Itinerant Electron Magnetism*, Springer-Verlag, Berlin (1998); A. J. Mills, *Phys. Rev. B* **48**, 7183 (1993).
10. S.-S. Lee, *Phys. Rev. B* **80**, 165102 (2009); M. A. Metlitski, S. Sachdev, *Phys. Rev. B* **82**, 075128 (2010).
11. S. Kasahara et al., *Phys. Rev. B* **81**, 184519 (2010).
12. Figure prepared by K. Jin, R. L. Greene, based on figure 56 in N. P. Armitage, P. Fournier, R. L. Greene, *Rev. Mod. Phys.* **82**, 2421 (2010).
13. R. A. Cooper et al., *Science* **323**, 603 (2009).
14. R. A. Borzi et al., *Science* **315**, 214 (2007).
15. V. Hinkov et al., *Science* **319**, 597 (2008); J.-H. Chu et al., *Science* **329**, 824 (2010).
16. L. Taillefer, *Annu. Rev. Condens. Matt. Phys.* **1**, 51 (2010).
17. S. A. Grigera et al., *Science* **294**, 329 (2001). ■